Rodrat, M., Jantarajit, W., Ng , D., Harvey, B. S. J., Liu, J., Wilkinson, W., Charoenphandhu, N., & Sheppard, D. N. (2020). Carbon monoxide-releasing molecules inhibit the cystic fibrosis transmembrane conductance regulator Cl- channel. *AJP - Lung Cellular and Molecular Physiology*, *319*(6), L997-L1009. https://doi.org/10.1152/ajplung.00440.2019

Carbon monoxide-releasing molecules inhibit the cystic fibrosis transmembrane conductance regulator Cl^- channel

Mayuree Rodrat,[1,2,3]* Walailak Jantarajit,[1,2,3]* Demi R. S. Ng,[1] Bartholomew S. J. Harvey,[1] Jia Liu,[1] William J. Wilkinson,[4] Narattaphol Charoenphandhu,[2,3,5,6] and David N. Sheppard[1]

[1] School of Physiology, Pharmacology and Neuroscience, University of Bristol, Bristol, UK,

[2] Center of Calcium and Bone Research (COCAB), Faculty of Science, Mahidol University, Bangkok, Thailand,

[3] Department of Physiology, Faculty of Science, Mahidol University, Bangkok, Thailand,

[4] School of Biosciences, Cardiff University, Cardiff, UK,

[5] Institute of Molecular Biosciences, Mahidol University, Nakhon Pathom, Thailand

and

[6] The Academy of Science, The Royal Society of Thailand, Dusit, Bangkok, Thailand

Running Title: Carbon monoxide-releasing molecules inhibit CFTR

*Author contributions: MR and WJ are co-first author

Address Correspondence to: D.N. Sheppard, Ph.D.
University of Bristol
School of Physiology, Pharmacology and Neuroscience
Biomedical Sciences Building
University Walk
Bristol BS8 1TD
United Kingdom
Tel: +44 117 331 2290
E-mail: D.N.Sheppard@bristol.ac.uk

ABSTRACT

The gasotransmitter carbon monoxide (CO) regulates fluid and electrolyte movements across epithelial tissues. However, its action on anion channels is incompletely understood. Here, we investigate the direct action of CO on the cystic fibrosis transmembrane conductance regulator (CFTR) by applying CO-releasing molecules (CORMs) to the intracellular side of excised inside-out membrane patches from cells heterologously expressing wild-type human CFTR. Addition of increasing concentrations of tricarbonyldichlororuthenium (II) dimer (CORM-2) (1 – 300 μM) inhibited CFTR channel activity, whereas the control $RuCl_3$ (100 μM) was without effect. CORM-2 predominantly inhibited CFTR by decreasing the frequency of channel openings and hence, open probability (P_o). But, it also reduced current flow through open channels with very fast kinetics, particularly at elevated concentrations. By contrast, the chemically distinct CO-releasing molecule CORM-3 inhibited CFTR by decreasing P_o without altering current flow through open channels. Neither depolarizing the membrane voltage nor raising the ATP concentration on the intracellular side of the membrane affected CFTR inhibition by CORM-2. Interestingly, CFTR inhibition by CORM-2, but not by $CFTR_{inh}$-172, was prevented by prior enhancement of channel activity by the clinically-approved CFTR potentiator ivacaftor. Similarly, when added after CORM-2, ivacaftor completely relieved CFTR inhibition. In conclusion, CORM-2 has complex effects on wild-type human CFTR consistent with allosteric inhibition and open-channel blockade. Inhibition of CFTR by CO-releasing molecules suggests that CO regulates CFTR activity and that the gasotransmitter has tissue-specific effects on epithelial ion transport. The action of ivacaftor on CFTR Cl^- channels inhibited by CO potentially expands the drug's clinical utility.

Keywords: CFTR chloride ion channel / channel inhibition / carbon monoxide-releasing molecule 2 (CORM-2) / CFTR potentiation / ivacaftor (VX-770)

INTRODUCTION

Widely expressed in epithelial cells lining ducts and tubes throughout the body, the cystic fibrosis transmembrane conductance regulator (CFTR) (56) plays a pivotal role in epithelia as testified by its dysfunction in the common life-shortening genetic disease cystic fibrosis (CF) (54, 58, 67). Assembled from two membrane-spanning domains (MSDs), two nucleotide-binding domains (NBDs) and a unique regulatory domain (RD) (56), CFTR (ABCC7) is an anion channel with the architecture of an ATP-binding cassette (ABC) transporter (22, 23, 36, 90). Once the RD is phosphorylated by protein kinase A (PKA) (45), CFTR gating is controlled by cycles of ATP binding and hydrolysis at the NBDs driving conformational changes in the MSDs, which open and close the channel pore (19, 23).

CFTR-mediated fluid and electrolyte movement across epithelial tissues involves the coordinated action of ion channels, transporters and pumps located in the apical and basolateral membranes of individual epithelial cells tightly regulated by a network of intracellular signaling pathways (18). It is now recognized that nitric oxide (NO), hydrogen sulfide (H_2S) and carbon monoxide (CO) act as endogenous gasotransmitters regulating the activity of ion channels and transporters in different tissues, including epithelia (1, 50, 85). Previous work demonstrates that NO and H_2S stimulate CFTR activity by modulating the phosphorylation status of CFTR. For example, in intestinal epithelial cells, NO robustly increases cGMP production (86). In turn, cGMP activates the membrane-localized type II cGMP-dependent protein kinase, leading to opening of the CFTR Cl^- channel (17, 71). By contrast, in *Xenopus* oocytes heterologously expressing CFTR, H_2S inhibits cAMP breakdown by phosphodiesterases to promote CFTR activation by PKA (49). Less is known about the regulation of CFTR by CO. With the Ussing chamber technique, two studies demonstrated that the CO-releasing molecule tricarbonyldichlororuthenium (II) dimer

(CORM-2) stimulated Cl^- secretion by intestinal epithelia, in part, by activating anion channels located in the apical membrane (66, 70). Based on these and other data (77, 78), Wang (79) speculated that CO stimulates CFTR by relieving CFTR inhibition by Fe^{3+}.

In this study, we investigated the direct action of CO on the CFTR Cl^- channel. Using CORM-2 and excised inside-out membrane patches from cells heterologously expressing wild-type human CFTR, we studied the effects of CO on the single-channel behavior of CFTR. We discovered that CORM-2 has complex effects on CFTR, impeding channel gating and obstructing current flow through open channels with characteristics similar to those of allosteric inhibitors and open-channel blockers of CFTR. Of note, the action of CORM-2 on CFTR was abolished by ivacaftor, a CFTR-targeting drug used clinically to treat CF (53, 72). These results inform studies of the physiological role of CFTR and the therapeutic utility of ivacaftor.

METHODS

Cells and cell culture

For this study, we used mouse mammary epithelial (C127) cells stably expressing wild-type human CFTR (39). These cells were a generous gift of C. R. O'Riordan (Sanofi Genzyme). They were cultured and used as described previously (62).

Patch-clamp experiments

CFTR Cl^- channels were recorded in excised inside-out membrane patches using Axopatch 200A and 200B patch-clamp amplifiers and pCLAMP software (version 10.4) (all from Molecular Devices, San Jose, CA) as described previously (62). Unless otherwise indicated, the pipette (extracellular) solution contained (mM): 140 N-methyl-D-glucamine

(NMDG), 140 aspartic acid, 5 $CaCl_2$, 2 $MgSO_4$ and 10 N-tris[Hydroxymethyl]methyl-2-aminoethanesulphonic acid (TES), adjusted to pH 7.3 with Tris ([Cl^-], 10 mM). The bath (intracellular) solution contained (mM): 140 NMDG, 3 $MgCl_2$, 1 CsEGTA and 10 TES adjusted to pH 7.3 with HCl ([Cl^-], 147 mM; free [Ca^{2+}], < 10^{-8} M). Using a temperature-controlled microscope stage (Brook Industries, Lake Villa, IL), the temperature of the bath solution was maintained at 37 °C.

After excision of inside-out membrane patches, we clamped voltage at –50 mV and added the catalytic subunit of PKA (75 nM) and ATP (1 mM) to the intracellular solution within 5 minutes of membrane patch excision to activate CFTR Cl^- channels. To test the effects of CORM-2 and other small molecules on the single-channel behavior of wild-type CFTR, we reduced the ATP concentration to 0.3 mM before adding compounds to the intracellular solution in the continuous presence of ATP (0.3 mM) and PKA (75 nM). Once channel activity stabilized following compound addition, we acquired 3 – 8 minutes of single-channel data. Because of the difficulty of removing ivacaftor from the recording chamber (84), specific interventions were compared with the pre-intervention control period made with the same concentration of ATP and PKA, but without test small molecules. To minimize channel rundown, PKA and ATP were added to all intracellular solutions. To investigate the voltage-dependence of CFTR inhibition, we used symmetrical Cl^--rich solutions and stepped voltage from 0 mV to either –50 mV for 60 s or +50 mV for 30 s. We chose 30 s steps at +50 mV because this time interval was long enough to acquire sufficient transitions to quantify open probability (P_o), but short enough to prevent seal breakdown and loss of the excised inside-out membrane patch. We did not step voltage to voltages beyond ±50 mV because of the weak inward rectification of CFTR Cl^- currents at large positive voltage (7).

In this study, we used excised inside-out membrane patches containing ≤ 5 active channels. To determine channel number, we used the maximum number of simultaneous channel openings observed during an experiment (9). To minimize errors, we used experimental conditions that robustly potentiate channel activity and verified that recordings were of sufficient length to determine the correct number of channels (74).

Single-channel currents were acquired directly to computer hard disc after filtering at a corner frequency (f_c) of 500 Hz using an eight-pole Bessel filter (model F-900C/9L8L, Frequency Devices Inc., Ottawa, IL) and digitized at a sampling rate of 5 kHz using a DigiData 1440A interface (Molecular Devices) and pCLAMP software (version 10.4). For Figure 7, data were additionally digitally filtered at 100 Hz prior to analysis. To measure single-channel current amplitude (i), Gaussian distributions were fit to current amplitude histograms. For P_o measurements, lists of open- and closed-times were generated using a half-amplitude crossing criterion for event detection and dwell time histograms constructed as previously described (62); transitions < 1 ms were excluded from the analysis (eight-pole Bessel filter rise time ($T_{10\text{-}90}$) ~0.73 ms at f_c = 500 Hz) with the exception of Figure 7, where transitions < 4 ms were excluded. Histograms were fitted with one or more component exponential functions using the maximum likelihood method. To determine which component function fitted best, the log-likelihood ratio test was used and considered statistically significant at a value of 2.0 or greater (87). For burst analyses, we used a t_c (the time that separates interburst closures from intraburst closures) determined from closed time histograms [control, t_c = 18.8 ± 5.2 ms (n = 5); ivacaftor, t_c = 10.8 ± 4.4 ms (n = 5); ivacaftor + CORM-2, t_c = 11.1 ± 1.6 ms (n = 5); ivacaftor + CORM-2 + $CFTR_{inh}$-172, t_c = 24.1 ± 1.7 ms (n = 4)] (9). The mean interburst interval (T_{IBI}) was calculated using the equation (9):

$$P_o = T_b / (T_{MBD} + T_{IBI}), \quad \text{(Eq. 1)}$$

where, T_b = (mean burst duration) x (open probability within a burst). Mean burst duration (T_{MBD}) and open probability within a burst ($P_{o(burst)}$) were determined directly from experimental data using pCLAMP software. Only membrane patches that contained a single active channel were used for burst and kinetic analyses. For the purpose of illustration, single-channel records were filtered at 500 Hz and digitized at 5 kHz before file size compression by 5-fold data reduction.

Reagents

PKA purified from bovine heart was purchased from Calbiochem (Merck Chemicals Ltd., Nottingham, UK). Ivacaftor was purchased from Selleck Chemicals (Stratech Scientific Ltd., Newmarket, UK), while all other chemicals, including CORM-2, CORM-3, $RuCl_3$ and $CFTR_{inh}$-172 were supplied by Sigma-Aldrich Ltd. (now Merck Life Science UK Ltd.) (Gillingham, UK).

Stock solutions of ATP were prepared in intracellular solution directly before each experiment. Except for CORM-3, which was dissolved in deionized water, all other stock solutions were solubilized in DMSO before storage at –20 °C. Immediately before use, stock solutions were diluted to final concentrations with intracellular solution and, where necessary, the pH of the intracellular solution was readjusted to pH 7.3 to avoid pH-dependent changes in CFTR function (10). Precautions against light-sensitive reactions were observed when using test small molecules. DMSO was without effect on the single-channel behavior of CFTR (62). On completion of experiments, the recording chamber was thoroughly cleaned before re-use (84).

Statistics

Data recording and analyses were randomized, but not blinded. Results are expressed as means ± SEM of *n* observations, but some group sizes were unequal due to technical difficulties with the acquisition of single-channel data. All data were tested for normal distribution using a Shapiro-Wilk normality test. To test for differences between two groups of data acquired within the same experiment, we used Student's paired *t*-test. To test for differences between multiple groups of data, we used one-way, repeated measures analysis of variance (ANOVA) followed by either Dunnett's or Tukey multiple comparison test when a statistically significant difference was observed. Tests were performed using SigmaPlot™ (version 13.0, Systat Software Inc., San Jose, CA) with the exception that concentration-response relationships were analyzed using Prism (version 5.0, GraphPad Software, San Diego, CA). Differences were considered statistically significant when $P < 0.05$. In patch-clamp experiments, *n* represents the number of individual membrane patches obtained from different cells. To avoid pseudo-replication, all experiments were repeated at different times.

Data accessibility statement

Data are available at the University of Bristol data repository, data.bris, at https://doi.org/10.5523/bris.12vo5en267fwo2x22o6afcxii1.

RESULTS

Carbon monoxide-releasing molecules inhibit wild-type CFTR

In this study, we investigated the direct action of CORM-2 on wild-type human CFTR using cell-free membrane patches from cells heterologously expressing CFTR. Following CFTR activation by PKA-dependent phosphorylation, we acutely added increasing

concentrations of CORM-2 to the intracellular solution in the continuous presence of PKA (75 nM) and ATP (0.3 mM). Figure 1 demonstrates that CORM-2 inhibited the activity of wild-type CFTR in two ways. First, CORM-2 altered the gating pattern of CFTR. The gating behavior of wild-type human CFTR is characterized by bursts of channel openings interrupted by brief, flickery closures, separated by longer closures between bursts (Fig. 1*A*). Addition of CORM-2 to the intracellular solution predominantly decreased the frequency of channel openings, but at higher concentrations, it also decreased markedly the duration of channel openings (Fig. 1). Second, CORM-2 altered current flow through open channels. Figure 1*A* and *B* demonstrate that elevated concentrations of CORM-2 decreased notably the single-channel current amplitude (*i*) of wild-type CFTR. To quantify channel inhibition by CORM-2, we measured *i* and P_o. Figure 1*C* and *D* show the effects of raising the CORM-2 concentration from 1 to 300 μM on the *i* and P_o of wild-type CFTR at –50 mV. For both *i* and P_o, the relationship between drug concentration and CFTR inhibition was well fitted by nonlinear regression functions with the effect of CORM-2 on P_o stronger than its action on *i* (*i*: IC_{50} = 46.8 ± 1.7 μM; P_o: IC_{50} = 31.0 ± 1.6 μM; *n* = 6 – 17) (Fig. 1*C* and *D*). Channel inhibition by CORM-2 was partially reversible (*n* = 3; data not shown). Thus, CORM-2 has complex effects on the CFTR Cl^- channel.

The chemical structure of the metal carbonyl complex CORM-2 (tricarbonyldichlororuthenium (II) dimer) is distinct from those of small molecules that inhibit the CFTR Cl^- channel (33, 41). As controls, we tested the effects on wild-type human CFTR of $RuCl_3$ and tricarbonylchloro(glycinato)ruthenium (II) (CORM-3), a CO-releasing molecule with a distinct chemical structure, which like CORM-2 rapidly releases CO (11, 41, 43). Figure 2 demonstrates that acute addition of $RuCl_3$ (100 μM) to the intracellular solution bathing excised inside-out membrane patches was without effect on the CFTR Cl^- channel.

Neither current flow through open channels nor channel gating and hence, P_o were affected by exposure to $RuCl_3$ (100 μM) (Fig. 2). By contrast, Figure 3 demonstrates that acute addition of CORM-3 (30 – 300 μM) to the intracellular solution inhibited wild-type CFTR. Comparison of the data in Figures 1 and 3 reveals two important differences between the two CO-releasing molecules. First, unlike CORM-2, CORM-3 was without effect on *i*; it only inhibited P_o by delaying channel opening (Figs. 1 and 3). Second, CORM-3 inhibited wild-type CFTR less potently than CORM-2 (Figs. 1*D* and 3*D*). It was also less efficacious than the widely used CFTR inhibitor $CFTR_{inh}$-172, an allosteric inhibitor of channel gating (31, 38) (Fig. 3). Taken together, the data demonstrate that acute addition of CO-releasing molecules to the intracellular solution directly inhibits the CFTR Cl^- channel. They also reveal that CORM-2 and CORM-3 impede channel opening and that CORM-2 additionally obstructs current flow through open channels.

Mechanistic studies of CORM-2 inhibition of wild-type CFTR

To understand better how CORM-2 inhibits wild-type human CFTR, we selected for study the concentration of 30 μM, close to the IC_{50} for CORM-2 inhibition of P_o. Using membrane patches containing a single active CFTR Cl^- channel, we investigated how CORM-2 decreased P_o by analyzing the kinetics of channel gating. Consistent with previous results [e.g. (87)], the open- and closed-time histograms of wild-type human CFTR were best fitted with one- and two-component exponential functions (Fig. 4*A* and Table 1). In this study, the two populations of channel closures described by fast (τ_{C2}) and slow (τ_{C3}) closed time constants, represent the brief, flickery closures that interrupt channel openings and the prolonged closures, which separate one burst of channel opening from the next.

In the presence of CORM-2 (30 μM) open- and closed-time histograms of wild-type human CFTR were best fitted with two- and four-component exponential functions, respectively (Fig. 4*B* and Table 1). The new population of open times was described by a fast open-time constant (τ_{O1}), while the new populations of closed times, which represent CORM-2-induced channel inhibition, were described by very fast (τ_{C1}) and very slow (τ_{C4}) closed-time constants (Fig. 4*B* and Table 1). In addition, CORM-2 (30 μM) increased the fast closed-time constant (τ_{C2}) by 58%, reduced the slow closed-time constant (τ_{C3}) by 41%, but was without effect on the slow open-time constant (τ_{O2}) (Fig. 4*B* and Table 1). Table 1 reveals that the share of the closed time distribution occupied by the fast (τ_{C2}) and slow (τ_{C3}) closed-time constants decreased by 38% and 14%, respectively in the presence of CORM-2 (30 μM). As a result, the new closed-time constants τ_{C1} and τ_{C4} occupied 51% and only 1% of the closed time distribution (Table 1). Interestingly, in the presence of CORM-2 (30 μM) the fast open time constant (τ_{O1}) dominated the open time distribution (Table 1). We interpret these data to suggest that CORM-2 has complex effects on the gating kinetics of CFTR, exhibiting similarities to the action of elevated concentrations of the CFTR potentiator genistein, which inhibits wild-type human CFTR (32).

Like genistein (32), the complex effects of CORM-2 on the CFTR Cl^- channel have characteristics in common with both open-channel blockers, which occlude the channel pore, and allosteric inhibitors that impede channel gating (23, 33). To probe the mechanism of CORM-2 inhibition of wild-type CFTR, we tested the effects of voltage and varied the intracellular ATP concentration. Many open-channel blockers occlude the intracellular vestibule of the CFTR pore, leading to voltage-dependent block (33, 35). For example, when bathed in symmetrical Cl^--rich solutions, glibenclamide (50 μM) potently inhibited wild-type CFTR at negative voltages, but at positive voltages inhibition was completely relieved (62).

Figure 5*A* shows a similar experiment using a membrane patch with two CFTR Cl^- channels bathed in symmetrical Cl^--rich solutions in the absence and presence of CORM-2 (30 μM) and summary data from six experiments. Under control conditions, the single-channel behavior of wild-type CFTR was unaffected by voltage; neither *i* nor P_o differed between –50 and +50 mV (Fig. 5*B* and *C*). Acute addition of CORM-2 (30 μM) to the intracellular solution potently inhibited channel gating at both voltages with the result that only brief openings of one channel were observed and P_o was strongly reduced at both voltages ($P_{o(drug)}/P_{o(control)}$: –50 mV, 29.0 ± 7.1% (*n* = 6); +50 mV, 23.0 ± 8.2% (*n* = 6); *P* = 0.16) (Fig. 5*A* and *C*). Although visual inspection of single-channel recordings indicates that some channel openings were of reduced size at both voltages in the presence of CORM-2 (30 μM), the summary data reveal no change in *i* at either voltage in the presence of CORM-2 (30 μM) ($i_{drug}/i_{control}$: –50 mV, 96.0 ± 3% (*n* = 6); +50 mV, 95.1 ± 3.0% (n = 6); *P* = 0.74) (Fig. 5*A* and *B*). We interpret these data to suggest that inhibition of wild-type CFTR by CORM-2 is voltage-independent, but its effect on current flow through open channels exhibits some dependence on the external Cl^- concentration based on the different effects of CORM-2 on *i* using either a Cl^- concentration gradient or symmetrical Cl^--rich solutions.

Allosteric inhibitors bind to CFTR at a site remote from the channel pore to interfere with channel gating (23, 33). Because some allosteric inhibitors [e.g. genistein (32)] interfere with ATP-dependent channel gating, we examined the effects of increasing the intracellular ATP concentration on CORM-2 inhibition of wild-type CFTR. Figure 6 shows representative single-channel recordings of wild-type CFTR using a Cl^- concentration gradient to demonstrate the effects of CORM-2 (30 μM) when the intracellular solution contained either 0.3 or 3 mM ATP and summary data from six to eight experiments. Consistent with previous results [e.g. (8)], elevating the ATP concentration to 3 mM noticeably increased the frequency

of channel openings and hence P_o, but had little or no effect on i (Fig. 6). However, raising the ATP concentration to 3 mM failed to relieve CFTR inhibition by CORM-2 (30 μM) (Fig. 6). At ATP (3 mM), the CORM-2-induced reductions in i and P_o were similar to those at ATP (0.3 mM) ($i_{drug}/i_{control}$: ATP (0.3 mM), 77.9 ± 6.8% (n = 8); ATP (3 mM), 87.6 ± 6.6% (n = 6); P = 0.28; $P_{o(drug)}/P_{o(control)}$: ATP (0.3 mM), 46.5 ± 12.2% (n = 8); ATP (3 mM), 46.1 ± 15.2% (n = 6); P = 0.8) (Fig. 6*C* and *D*). Taken together the data demonstrate that CORM-2 does not cause voltage-dependent inhibition of wild-type CFTR nor does it inhibit channel activity by competing with ATP.

Ivacaftor prevents CFTR inhibition by CORM-2

Previous work demonstrated that the clinically-approved CFTR potentiator ivacaftor (53, 72) relieves CFTR inhibition by cigarette smoke (52). We were therefore interested to learn whether ivacaftor would modify the inhibition of wild-type CFTR by CORM-2. To test this idea, we performed two experiments, acutely adding both compounds to the intracellular solution bathing excised membrane patches from cells heterologously expressing wild-type CFTR; first we added ivacaftor (100 nM) before CORM-2 (30 μM) and second, we reversed the order of addition of the two compounds.

Figure 7 shows the effects of sequential and cumulative addition of CORM-2 (30 μM) and $CFTR_{inh}$-172 (10 μM) on a single wild-type CFTR Cl^- channel potentiated by ivacaftor (100 nM). To quantify the data, we measured i, P_o and performed an analysis of bursts to determine how small molecules alter the frequency and duration of channel openings. Consistent with previous results [e.g. (83)], acute addition of ivacaftor (100 nM) to the intracellular solution potentiated CFTR channel gating by increasing the frequency and duration of channel openings, leading to an 66% increase in P_o, but no change in i (Fig. 7).

Figure 7 demonstrates that once wild-type CFTR was potentiated by ivacaftor (100 nM), CORM-2 (30 μM) was without effect on current flow through open channels and had little or no effect on the pattern of channel gating. Neither *i*, mean burst duration (MBD) nor interburst interval (IBI) were altered by the small molecule, while P_o was reduced only 18% compared to that potentiated by ivacaftor (100 nM) (Fig. 7). By contrast, subsequent addition of $CFTR_{inh}$-172 (10 μM) had a marked effect on channel gating, increasing IBI 2,035% and reducing MBD 52% without altering *i* (Fig. 7). These effects of $CFTR_{inh}$-172 (10 μM) after CORM-2 (30 μM) closely resemble its action on wild-type CFTR potentiated by ivacaftor (100 nM) in the absence of CORM-2 (25).

Finally, we tested whether ivacaftor would relieve the inhibition of wild-type CFTR by CORM-2. Figure 8 shows that CORM-2 (30 μM) reduced *i* 10% and P_o 57%. However, subsequent acute addition of ivacaftor (100 nM) to the intracellular solution restored values of *i* and P_o to control levels before CORM-2 (30 μM) exposure (Fig. 8). Like its effect after ivacaftor and CORM-2 (Fig. 7), the ensuing addition of $CFTR_{inh}$-172 (10 μM) to the intracellular solution strongly inhibited the P_o of wild-type CFTR, without altering *i* (Fig. 8). Thus, like its effects on CFTR inhibition by cigarette smoke (52), ivacaftor prevents wild-type CFTR inhibition by CORM-2.

DISCUSSION

This study investigated the direct action of CORM-2 on wild-type human CFTR using the patch-clamp technique. Our data demonstrate that CORM-2 impedes channel gating and obstructs current flow through CFTR. However, its action is abolished by the clinically-approved CFTR potentiator ivacaftor.

The present results contrast with previous studies of CORM-2 on transepithelial ion transport with the Ussing chamber technique, which demonstrated that the small molecule activated anion channels in the apical membrane of cultured human intestinal (Caco-2) and rat colonic epithelia (66, 70). Using similar concentrations of CORM-2, we only observed inhibition of the CFTR Cl^- channel. Moreover, we found no evidence for dual effects, unlike some CFTR modulators, which either potentiate or inhibit channel activity depending on the experimental conditions employed [e.g. genistein (32, 76); NPPB (34, 82); phloxine B (8)]. Species differences in CFTR pharmacology [e.g. (4, 65)] is an unlikely explanation for the results obtained. By contrast, variation in the complement of transport proteins, signaling molecules and CFTR-interacting proteins in the different cells used to study CFTR [Caco-2 cells (70); rat distal colon (66); C127 cells (present study)] is a potential explanation. Similarly, using cell-free membrane patches, cytosolic regulatory factors might be lost, whereas in polarized intestinal epithelia they would be retained (66, 70) and the present study).

However, the most likely explanation for the different results is the action of CO on distinct types of apical membrane anion channels. Under the experimental conditions used by Uc et al. (70) and Steidle and Diener (66), it is feasible that the inhibitors DIDS, glibenclamide and NPPB might have decreased short-circuit current (I_{sc}) by targeting other anion channels, not CFTR. Consistent with this idea, in rat epididymal epithelia, the NPPB- and DIDS-sensitive CORM-2-induced increase in I_{sc} was robustly inhibited by chelation of intracellular Ca^{2+} with BAPTA-AM, whereas the CFTR inhibitor $CFTR_{inh}$-172 had little effect (48). These data suggest that in rat epididymal epithelia CORM-2 increases I_{sc} by targeting the Ca^{2+}-activated Cl^- channel TMEM16A (47). Interestingly, CORM-2 and CORM-3 inhibited cAMP signaling and cAMP-stimulated I_{sc} in cultured human bronchial

386 epithelia (16HBE14o$^-$) (89), while hypercapnia had similar effects on primary cultures of
387 human airway epithelia (69).
388
389 We found that two CO-releasing molecules, CORM-2 and CORM-3, acutely inhibited
390 the CFTR Cl^- channel in excised inside-out membrane patches, whereas $RuCl_3$ was without
391 effect. Because the biological activity of CORM-2 and CORM-3 is directly related to CO
392 (11, 42), the simplest interpretation of the data is that CO inhibits CFTR. However, the
393 diverse chemical structures of CFTR inhibitors (33) cautions that the CO-releasing molecules,
394 themselves, not CO, might mediate the observed effects. Interestingly, CORM-2, a lipid
395 soluble CO-releasing molecule (41), inhibited CFTR with greater potency and efficacy than
396 CORM-3, a water-soluble compound (11). We interpret these results to suggest that the
397 action of CO-releasing molecules involves the lipid bilayer or the MSDs of CFTR, which
398 interact with it. Consistent with this idea, ivacaftor, prevented CFTR inhibition by CORM-2,
399 but not $CFTR_{inh}$-172. Interestingly, ivacaftor binds CFTR at the MSD-lipid interface with
400 residues from the fourth transmembrane segment (M4), M5 and the unstructured region of M8
401 contributing to this potentiator-binding pocket (37, 88). Carbon monoxide might compete
402 with ivacaftor for binding to this site. Alternatively, the interaction of ivacaftor with this site
403 might modulate allosterically the interaction of CO with CFTR. In support of this latter idea,
404 ivacaftor promotes occupancy of the open channel configuration, providing an explanation for
405 its rescue of CF mutants located throughout the structure of CFTR (26, 27, 73).
406
407 Previous work has identified two general mechanisms of CFTR inhibition: open-
408 channel blockade and allosteric inhibition (23, 33, 35). Open-channel blockers, such as
409 glibenclamide and GlyH-101, occlude the vestibules of the CFTR pore, leading to voltage-
410 dependent block (44, 62). By contrast, allosteric inhibitors, such as $CFTR_{inh}$-172 and (*R*)-

411 BPO-27 interfere with channel gating (30, 31). Like genistein and thyroid hormones (6, 32),
412 CORM-2 had complex effects on the single-channel behavior of CFTR, exhibiting
413 characteristics of both allosteric inhibition and open-channel blockade. It principally
414 inhibited CFTR by slowing channel gating, influencing gating kinetics in a similar manner to
415 elevated concentrations of genistein (32). However, unlike genistein and (*R*)-BPO-27 (30,
416 32), elevating the ATP concentration failed to relieve CFTR inhibition. This result suggests
417 that like $CFTR_{inh}$-172 (31), CORM-2 interferes with channel gating at a different location
418 within the CFTR gating pathway, the wave of conformational changes initiated by ATP
419 binding at the NBD1:NBD2 interface, which lead to opening of the channel pore (13, 64). As
420 indicated above, CORM-2 might exert its effects on channel gating at the ivacaftor-binding
421 site (37, 88). This site is distinct from the $CFTR_{inh}$-172-binding site, which involves R347, a
422 non-pore lining residue within M6 (5, 23).
423
424 The CORM-2-induced reduction in *i* has characteristics of "very fast" open-channel
425 block of CFTR resembling the kinetics of CFTR inhibition by niflumic acid and furosemide
426 (28, 59). However, like elevated concentrations of genistein (32), CORM-2 inhibition of
427 CFTR was voltage-independent. One possibility is that CORM-2 exerts its effects on CFTR
428 by interacting with multiple binding sites. Consistent with this idea, we interpreted the
429 inhibitory effects of genistein on channel gating and current flow to involve its interaction
430 with two sites on CFTR: the NBDs and the intracellular vestibule of the channel pore (32).
431 However, the location of the ivacaftor-binding site (37, 88) raises the interesting possibility
432 that CORM-2 might impede channel gating and anion movement through CFTR by
433 interaction with a single site located in a pivotal position within the MSDs.
434

435 The mechanism of CFTR inhibition by CORM-2 appears distinct from its actions on
436 other ion channels. Previous work demonstrates that CORM-2 regulates ion channels by
437 direct and indirect mechanisms [for review, see (85)]. Direct mechanisms include CO
438 binding to histidine residues [e.g. (80)] and a high-affinity, channel-associated heme moiety
439 [e.g. (24)]. Indirect mechanisms include CO-dependent generation of cGMP [e.g. (55)],
440 similar to the action of NO (1) and modulation of the cellular redox state [e.g. (60)]. The
441 former mechanism would be expected to active CFTR in intestinal epithelial cells (17, 71),
442 but studies using inhibitors of cGMP signaling have proved inconclusive (66, 70).
443 Interestingly, Kapetanaki et al. (29) demonstrated that CO activation of ATP-sensitive K^+
444 channels involves heme binding to a $CXXHX_{16}H$ motif on sulphonylurea receptor 2A, an
445 ABC transporter closely related to CFTR. The authors showed that CFTR lacks this heme-
446 binding motif. Similarly, the ivacaftor-binding site (37, 88) lacks amino acid residues
447 previously demonstrated to interact with CO (80), raising the possibility of CO directly
448 regulates CFTR at a different site or by a different mechanism.
449
450 This work has several potential caveats. First, we did not test the effects of CO gas on
451 CFTR. Instead, we used the CO-releasing molecules CORM-2 and CORM-3 and found that
452 they had distinct inhibitory effects. As discussed above, although it is well established that
453 the biological activity of CO-releasing molecules is mediated by CO (41, 43), our data do not
454 exclude the possibility that the CO-releasing molecules, themselves, not CO, inhibit CFTR.
455 Second, we did not measure CO generation by CORM-2 and CORM-3. However, we used
456 both CO-releasing molecules at concentrations equivalent to those employed in previous
457 studies of CO's action on epithelial anion transport (48, 66, 70, 89) and demonstrated to
458 liberate CO similar to the original descriptions of these agents (CORM-2: 0.7 mole CO per
459 mole CORM-2; CORM-3: 1 mole CO per mole CORM-3) (11, 42, 89). Although the CO

concentration in epithelial cells is difficult to determine (66), these concentrations are similar to those estimated for endogenous CO production by humans under physiological conditions (~18 μmole CO h^{-1}) (12, 57). Third, we examined the direct effects of CO-releasing molecules on the single-channel activity of CFTR. We did not study their action on a large population of CFTR Cl^- channels. In previous work, we have demonstrated that the single-channel behavior of CFTR provides molecular explanations for quantitative changes in CFTR-mediated transepithelial Cl^- currents caused by CF variants [e.g. (61)] and small molecules [e.g. (59)]. Although a further limitation of this work is the use of C127 cells heterologously expressing CFTR, single-channel studies of epithelial cells endogenously expressing human CFTR are highly challenging preventing their routine use.

There are several important implications of the present study. First, the present data and previous results (66, 70, 89) suggest that CO might be a physiological regulator of CFTR function. The CO producing enzymes heme oxygenase-1 (HO-1) and -2 are expressed in epithelial tissues (66, 89). Of note, HO-1 is a modifier gene for *Pseudomonas aeruginosa* infection in CF (46), while in macrophages ezrin appears to assemble HO-1 and CFTR into a macromolecular signaling complex (15, 20). However, the action of CO appears to be tissue-specific, stimulating Cl^- secretion in the intestine (66, 70) and epididymis (48), Na^+ absorption in the kidney (81), but inhibiting ion transport in the lung (2, 89). These distinct effects of CO on epithelial ion transport might be explained by differences in the redox status of cells (85).

Second, the present results and other data (2) suggest that CO should be used with caution to treat lung inflammation. Based on its wide ranging beneficial effects, including dampening inflammation, reducing oxidative stress and strengthening host defense

485 mechanisms [for review, see (14, 43)], CO has been investigated as a therapy for lung
486 inflammation in acute respiratory distress syndrome (16) and chronic obstructive pulmonary
487 disease (COPD) (3). Like COPD (51), CF lung disease is characterized by persistent bacterial
488 infection and exaggerated inflammatory responses (54). Although CO has been proposed as
489 an adjuvant therapy for CF lung disease (14), our observation that CORM-2 potently inhibits
490 CFTR cautions that great care should be exercised with its use because of the adverse effects
491 on host defense mechanisms of CFTR inhibition (67).
492
493 Third, the present results potentially expand the clinical utility of ivacaftor. Currently,
494 ivacaftor is used to treat CF patients with some gating mutations [e.g. G551D; (53)] and in
495 combination with lumacaftor or tezacaftor and elexacaftor, CF patients with the F508del
496 mutation (21, 40, 68, 75). Raju et al. (52) demonstrated that ivacaftor abrogates acquired
497 CFTR inhibition by cigarette smoke, suggesting that the drug might be used to treat COPD
498 and other smoking-related diseases (63). Building on this study, the present results suggest
499 that ivacaftor might be used to alleviate CO poisoning caused environmental pollution.
500
501 In conclusion, this study demonstrates that the CO-releasing molecules CORM-2 and
502 CORM-3 inhibit the CFTR Cl^- channel. CORM-2 and CORM-3 predominantly act as
503 allosteric inhibitors, slowing the rate of channel opening. But, additionally, CORM-2
504 impeded current flow through open channels with very fast kinetics. Of note, the clinically-
505 approved CFTR potentiator ivacaftor abolished CFTR inhibition by CORM-2. Building on
506 other studies (48, 66, 70, 89), the present work suggests that CO might be a physiological
507 regulator of CFTR-mediated epithelial ion transport. The current data and those of Raju et al.
508 (52) also argue that ivacaftor has wider clinical utility than the treatment of CF.
509

AUTHOR CONTRIBUTIONS

Conception and design of the experiments: W.J.W., N.C. and D.N.S.; performed the research: M.R., W.J., D.R.S.N., B.S.J.H. and J.L.; analysis and interpretation of data: M.R., W.J., D.R.S.N., B.S.J.H., J.L., W.J.W., N.C. and D.N.S.; drafting the article or revising it critically for important intellectual content: M.R., W.J., W.J.W., N.C. and D.N.S.. All authors approved the final version of the manuscript.

CONFLICT OF INTEREST

The authors declare that they have no conflicts of interest with the contents of this manuscript.

ACKNOWLEDGEMENTS

We thank CR O'Riordan for the generous gift of heterologous cells and our laboratory colleagues for valuable discussions and assistance. This work was supported by the Cystic Fibrosis Trust. MR, WJ and NC were supported by Mahidol University-Multidisciplinary Research Center grant and the Thailand Research Fund (International Research Network Program [IRN60W0001] and Senior Research Scholar Grant [RTA6080007]). MR and WJ were recipients of scholarships from The Royal Golden Jubilee PhD programme, co-funded by the Thailand Research Fund and the UK Newton Fund (WJ: PHD/0084/2554; MR: PHD/0105/2557).

AUTHOR'S PRESENT ADDRESSES

W. J. Wilkinson: Beechen Cliff School, Kipling Avenue, Bath BA2 1HL, UK

REFERENCES

1. **Althaus M.** Gasotransmitters: novel regulators of epithelial Na^+ transport? *Front Physiol* 3: 83, 2012.

2. **Althaus M, Fronius M, Buchäckert Y, Vadász I, Clauss WG, Seeger W, Motterlini R, Morty RE.** Carbon monoxide rapidly impairs alveolar fluid clearance by inhibiting epithelial sodium channels. *Am J Respir Cell Mol Biol* 41: 639-650, 2009.

3. **Bathoorn E, Slebos DJ, Postma DS, Koeter GH, van Oosterhout AJM, van der Toorn M, Boezen HM, Kerstjens HAM.** Anti-inflammatory effects of inhaled carbon monoxide in patients with COPD: a pilot study. *Eur Respir J* 30: 1131-1137, 2007.

4. **Bose SJ, Bijvelds MJC, Wang Y, Liu J, Cai Z, Bot AGM, de Jonge HR, Sheppard DN.** Differential thermostability and response to cystic fibrosis transmembrane conductance regulator potentiators of human and mouse F508del-CFTR. *Am J Physiol Lung Cell Mol Physiol* 317: L71-L86, 2019.

5. **Caci E, Caputo A, Hinzpeter A, Arous N, Fanen P, Sonawane N, Verkman AS, Ravazzolo R, Zegarra-Moran O, Galietta LJV.** Evidence for direct CFTR inhibition by $CFTR_{inh}$-172 based on Arg^{347} mutagenesis. *Biochem J* 413: 135-142, 2008.

6. **Cai Z, Li H, Chen JH, Sheppard DN.** Acute inhibition of the cystic fibrosis transmembrane conductance regulator (CFTR) Cl^- channel by thyroid hormones involves multiple mechanisms. *Am J Physiol Cell Physiol* 305: C817-C828, 2013.

7. **Cai Z, Scott-Ward TS, Sheppard DN.** Voltage-dependent gating of the cystic fibrosis transmembrane conductance regulator Cl^- channel. *J Gen Physiol* 122: 605-620, 2003.

8. **Cai Z, Sheppard DN.** Phloxine B interacts with the cystic fibrosis transmembrane conductance regulator at multiple sites to modulate channel activity. *J Biol Chem* 277: 19546-19553, 2002.

9. **Cai Z, Taddei A, Sheppard DN.** Differential sensitivity of the cystic fibrosis (CF)-associated mutants G551D and G1349D to potentiators of the cystic fibrosis transmembrane conductance regulator (CFTR) Cl^- channel. *J Biol Chem* 281: 1970-1977, 2006.

10. **Chen JH, Cai Z, Sheppard DN.** Direct sensing of intracellular pH by the cystic fibrosis transmembrane conductance regulator (CFTR) Cl^- channel. *J Biol Chem* 284: 35495-35506, 2009.

11. **Clark JE, Naughton P, Shurey S, Green CJ, Johnson TR, Mann BE, Foresti R, Motterlini R.** Cardioprotective actions by a water-soluble carbon monoxide-releasing molecule. *Circ Res* 93: e2-e8, 2003.

12. **Coburn RF, Blakemore WS, Forster RE.** Endogenous carbon monoxide production in man. *J Clin Invest* 42: 1172-1178, 1963.

13. **Csanády L, Nairn AC, Gadsby DC.** Thermodynamics of CFTR channel gating: a spreading conformational change initiates an irreversible gating cycle. *J Gen Physiol* 128: 523-533, 2006.

14. **Di Pietro C, Öz HH, Murray TS, Bruscia EM.** Targeting the heme oxygenase 1/carbon monoxide pathway to resolve lung hyper-inflammation and restore a regulated immune response in cystic fibrosis. *Front Pharmacol* 11: 1059, 2020.

15. **Di Pietro C, Zhang P-x, O'Rourke TK, Murray TS, Wang L, Britto CJ, Koff JL, Krause DS, Egan ME, Bruscia EM.** Ezrin links CFTR to TLR4 signaling to orchestrate anti-bacterial immune response in macrophages. *Sci Rep* 7: 10882, 2017.

16. **Fredenburgh LE, Perrella MA, Barragan-Bradford D, Hess DR, Peters E, Welty-Wolf KE, Kraft BD, Harris RS, Maurer R, Nakahira K, Oromendia C, Davies JD, Higuera A, Schiffer KT, Englert JA, Dieffenbach PB, Berlin DA, Lagambina S, Bouthot M, Sullivan AI, Nuccio PF, Kone MT, Malik MJ, Porras MAP, Finkelsztein E, Winkler T, Hurwitz S, Serhan CN, Piantadosi CA, Baron RM, Thompson BT, Choi AMK.** A phase I trial of low-dose inhaled carbon monoxide in sepsis-induced ARDS. *JCI Insight* 3: e124039, 2018.

17. **French PJ, Bijman J, Edixhoven M, Vaandrager AB, Scholte BJ, Lohmann SM, Nairn AC, de Jonge HR.** Isotype-specific activation of cystic fibrosis transmembrane conductance regulator-chloride channels by cGMP-dependent protein kinase II. *J Biol Chem* 270: 26626-26631, 1995.

18. **Frizzell RA, Hanrahan JW.** Physiology of epithelial chloride and fluid secretion. *Cold Spring Harb Perspect Med* 2: a009563, 2012.

19. **Gadsby DC, Vergani P, Csanády L.** The ABC protein turned chloride channel whose failure causes cystic fibrosis. *Nature* 440: 477-483, 2006.

20. **Guggino WB, Stanton BA.** New insights into cystic fibrosis: molecular switches that regulate CFTR. *Nat Rev Mol Cell Biol* 7: 426-436, 2006.

21. **Harutyunyan M, Huang Y, Mun K-S, Yang F, Arora K, Naren AP.** Personalized medicine in CF: from modulator development to therapy for cystic fibrosis patients with rare CFTR mutations. *Am J Physiol Lung Cell Mol Physiol* 314: L529-L543, 2018.

22. **Holland IB, Cole SPC, Kuchler K, Higgins CF.** *ABC Proteins: from bacteria to man*. London: Academic Press, 2003.

23. **Hwang TC, Yeh JT, Zhang J, Yu YC, Yeh HI, Destefano S.** Structural mechanisms of CFTR function and dysfunction. *J Gen Physiol* 150: 539-570, 2018.

24. **Jaggar JH, Li A, Parfenova H, Liu J, Umstot ES, Dopico AM, Leffler CW.** Heme is a carbon monoxide receptor for large-conductance Ca^{2+}-activated K^+ channels. *Circ Res* 97: 805-812, 2005.

25. **Jantarajit W, Wongdee K, Lertsuwan K, Teerapornpuntakit J, Aeimlapa R, Thongbunchoo J, Harvey BSJ, Sheppard DN, Charoenphandhu N.** Parathyroid

hormone increases CFTR expression and function in Caco-2 intestinal epithelial cells. *Biochem Biophys Res Commun* 523: 816-821, 2020.

26. **Jih KY, Hwang TC.** Vx-770 potentiates CFTR function by promoting decoupling between the gating cycle and ATP hydrolysis cycle. *Proc Natl Acad Sci USA* 110: 4404-4409, 2013.

27. **Jih KY, Lin WY, Sohma Y, Hwang TC.** CFTR potentiators: from bench to bedside. *Curr Opin Pharmacol* 34: 98-104, 2017.

28. **Ju M, Scott-Ward TS, Liu J, Khuituan P, Li H, Cai Z, Husbands SM, Sheppard DN.** Loop diuretics are open-channel blockers of the cystic fibrosis transmembrane conductance regulator with distinct kinetics. *Br J Pharmacol* 171: 265-278, 2014.

29. **Kapetanaki SM, Burton MJ, Basran J, Uragami C, Moody PCE, Mitcheson JS, Schmid R, Davies NW, Dorlet P, Vos MH, Storey NM, Raven E.** A mechanism for CO regulation of ion channels. *Nat Commun* 9: 907, 2018.

30. **Kim Y, Anderson MO, Park J, Lee MG, Namkung W, Verkman AS.** Benzopyrimido-pyrrolo-oxazine-dione (*R*)-BPO-27 inhibits CFTR chloride channel gating by competition with ATP. *Mol Pharmacol* 88: 689-696, 2015.

31. **Kopeikin Z, Sohma Y, Li M, Hwang TC.** On the mechanism of CFTR inhibition by a thiazolidinone derivative. *J Gen Physiol* 136: 659-671, 2010.

32. **Lansdell KA, Cai Z, Kidd JF, Sheppard DN.** Two mechanisms of genistein inhibition of cystic fibrosis transmembrane conductance regulator Cl^- channels expressed in murine cell line. *J Physiol* 524: 317-330, 2000.

33. **Li H, Sheppard DN.** Therapeutic potential of cystic fibrosis transmembrane conductance regulator (CFTR) inhibitors in polycystic kidney disease. *BioDrugs* 23: 203-216, 2009.

34. **Lin WY, Sohma Y, Hwang TC.** Synergistic potentiation of cystic fibrosis transmembrane conductance regulator gating by two chemically distinct potentiators, ivacaftor (VX-770) and 5-nitro-2-(3-phenylpropylamino) benzoate. *Mol Pharmacol* 90: 275-285, 2016.

35. **Linsdell P.** Cystic fibrosis transmembrane conductance regulator chloride channel blockers: pharmacological, biophysical and physiological relevance. *World J Biol Chem* 5: 26-39, 2014.

36. **Liu F, Zhang Z, Csanády L, Gadsby DC, Chen J.** Molecular structure of the human CFTR ion channel. *Cell* 169: 85-95, 2017.

37. **Liu F, Zhang Z, Levit A, Levring J, Touhara KK, Shoichet BK, Chen J.** Structural identification of a hotspot on CFTR for potentiation. *Science* 364: 1184-1188, 2019.

38. **Ma T, Thiagarajah JR, Yang H, Sonawane ND, Folli C, Galietta LJV, Verkman AS.** Thiazolidinone CFTR inhibitor identified by high-throughput screening blocks cholera toxin-induced intestinal fluid secretion. *J Clin Invest* 110: 1651-1658, 2002.

39. **Marshall J, Fang S, Ostedgaard LS, O'Riordan CR, Ferrara D, Amara JF, Hoppe H IV, Scheule RK, Welsh MJ, Smith AE, Cheng SH.** Stoichiometry of recombinant cystic fibrosis transmembrane conductance regulator in epithelial cells and its functional reconstitution into cells *in vitro*. *J Biol Chem* 269: 2987-2995, 1994.

40. **Middleton PG, Mall MA, Dřevínek P, Lands LC, McKone EF, Polineni D, Ramsey BW, Taylor-Cousar JL, Tullis E, Vermeulen F, Marigowda G, McKee CM, Moskowitz SM, Nair N, Savage J, Simard C, Tian S, Waltz D, Xuan F, Rowe SM, Jain, M; VX17-445-102 Study Group.** Elexacaftor-tezacaftor-ivacaftor for cystic fibrosis with a single Phe508del allele. *N Engl J Med* 381: 1809-1819, 2019.

41. **Motterlini R.** Carbon monoxide-releasing molecules (CO-RMs): vasodilatory, anti-ischaemic and anti-inflammatory activities. *Biochem Soc Trans* 35: 1142-1146, 2007.

42. **Motterlini R, Clark JE, Foresti R, Sarathchandra P, Mann BE, Green CJ.** Carbon monoxide-releasing molecules: characterization of biochemical and vascular activities. *Circ Res* 90: e17-e24, 2002.

43. **Motterlini R, Otterbein LE.** The therapeutic potential of carbon monoxide. *Nat Rev Drug Discov* 9: 728-743, 2010.

44. **Muanprasat C, Sonawane ND, Salinas D, Taddei A, Galietta LJV, Verkman AS.** Discovery of glycine hydrazide pore-occluding CFTR inhibitors: mechanism, structure-activity analysis and in vivo efficacy. *J Gen Physiol* 124: 125-137, 2004.

45. **Ostedgaard LS, Baldursson O, Welsh MJ.** Regulation of the cystic fibrosis transmembrane conductance regulator Cl^- channel by its R domain. *J Biol Chem* 276: 7689-7692, 2001.

46. **Park JE, Yung R, Stefanowicz D, Shumansky K, Akhabir L, Durie PR, Corey M, Zielenski J, Dorfman R, Daley D, Sandford AJ.** Cystic fibrosis modifier genes related to Pseudomonas aeruginosa infection. *Genes Immun* 12: 370-377, 2011.

47. **Pedemonte N, Galietta LJV.** Structure and function of TMEM16 proteins (anoctamins). *Physiol Rev* 94: 419-459, 2014.

48. **Peng L, Gao D-D, Xu J-W, Xu J-B, Ke L-J, Qiu Z-E, Zhu Y-X, Zhang Y-L, Zhou W-L.** Cellular mechanisms underlying carbon monoxide stimulated anion secretion in rat epididymal epithelium. *Nitric Oxide* 100-101: 30-37, 2020.

49. **Perniss A, Preiss K, Nier M, Althaus M.** Hydrogen sulfide stimulates CFTR in *Xenopus* oocytes by activation of the cAMP/PKA signalling axis. *Sci Rep* 7: 3517, 2017.

50. **Pouokam E, Steidle J, Diener M.** Regulation of colonic ion transport by gasotransmitters. *Biol Pharm Bull* 34: 789-793, 2011.

51. **Rab A, Rowe SM, Raju SV, Bebok Z, Matalon S, Collawn JF.** Cigarette smoke and CFTR: implications in the pathogenesis of COPD. *Am J Physiol Lung Cell Mol Physiol* 305: L530-L541, 2013.

52. **Raju SV, Lin VY, Liu L, McNicholas CM, Karki S, Sloane PA, Tang L, Jackson PL, Wang W, Wilson L, Macon KJ, Mazur M, Kappes JC, DeLucas LJ, Barnes S, Kirk K, Tearney GJ, Rowe SM.** The cystic fibrosis transmembrane conductance regulator potentiator ivacaftor augments mucociliary clearance abrogating cystic fibrosis transmembrane conductance regulator inhibition by cigarette smoke. *Am J Respir Cell Mol Biol* 56: 99-108, 2017.

53. **Ramsey BW, Davies J, McElvaney NG, Tullis E, Bell SC, Dřevínek P, Griese M, McKone EF, Wainwright CE, Konstan MW, Moss R, Ratjen F, Sermet-Gaudelus I, Rowe SM, Dong Q, Rodriguez S, Yen K, Ordoñez C, Elborn JS; VX08-770-102 Study Group.** A CFTR potentiator in patients with cystic fibrosis and the *G551D* mutation. *N Engl J Med* 365: 1663-1671, 2011.

54. **Ratjen F, Bell SC, Rowe SM, Goss CH, Quittner AL, Bush A.** Cystic fibrosis. *Nat Rev Dis Primers* 1: 15010, 2015.

55. **Rich A, Farrugia G, Rae JL.** Carbon monoxide stimulates a potassium-selective current in rabbit corneal epithelial cells. *Am J Physiol Cell Physiol* 267: C435-C442, 1994.

56. **Riordan JR, Rommens JM, Kerem BS, Alon N, Rozmahel R, Grzelczak Z, Zielenski J, Lok S, Plavsic N, Chou JL, Drumm ML, Iannuzzi MC, Collins FS, Tsui LC.** Identification of the cystic fibrosis gene: cloning and characterization of complementary DNA. *Science* 245: 1066-1073, 1989.

57. **Ryter SW, Choi AMK.** Carbon monoxide in exhaled breath testing and therapeutics. *J Breath Res* 7: 017111, 2013.

58. **Saint-Criq V, Gray MA.** Role of CFTR in epithelial physiology. *Cell Mol Life Sci* 74: 93-115, 2017.

59. **Scott-Ward TS, Li H, Schmidt A, Cai Z, Sheppard DN.** Direct block of the cystic fibrosis transmembrane conductance regulator Cl^- channel by niflumic acid. *Mol Membr Biol* 21: 27-38, 2004.

60. **Scragg JL, Dallas ML, Wilkinson JA, Varadi G, Peers C.** Carbon monoxide inhibits L-type Ca^{2+} channels via redox modulation of key cysteine residues by mitochondrial reactive oxygen species. *J Biol Chem* 283: 24412-24419, 2008.

61. **Sheppard DN, Ostedgaard LS, Winter MC, Welsh MJ.** Mechanism of dysfunction of two nucleotide binding domain mutations in cystic fibrosis transmembrane conductance regulator that are associated with pancreatic sufficiency. *EMBO J* 14: 876-883, 1995.

62. **Sheppard DN, Robinson KA.** Mechanism of glibenclamide inhibition of cystic fibrosis transmembrane conductance regulator Cl^- channels expressed in a murine cell line. *J Physiol* 503: 333-346, 1997.

63. **Solomon GM, Fu L, Rowe SM, Collawn JF.** The therapeutic potential of CFTR modulators for COPD and other airway diseases. *Curr Opin Pharmacol* 34: 132-139, 2017.

64. **Sorum B, Czégé D, Csanády L.** Timing of CFTR pore opening and structure of its transition state. *Cell* 163: 724-733, 2015.

65. **Stahl M, Stahl K, Brubacher MB, Forrest JN Jr.** Divergent CFTR orthologs respond differently to the channel inhibitors $CFTR_{inh}$-172, glibenclamide, and GlyH-101. *Am J Physiol Cell Physiol* 302: C67-C76, 2012.

66. **Steidle J, Diener M.** Effects of carbon monoxide on ion transport across rat distal colon. *Am J Physiol Gastrointest Liver Physiol* 300: G207-G216, 2011.

67. **Stoltz DA, Meyerholz DK, Welsh MJ.** Origins of cystic fibrosis lung disease. *N Engl J Med* 372: 351-362, 2015.

68. **Taylor-Cousar JL, Munck A, McKone EF, van der Ent CK, Moeller A, Simard C, Wang LT, Ingenito EP, McKee C, Lu Y, Lekstrom-Himes J, Elborn JS.** Tezacaftor-ivacaftor in patients with cystic fibrosis homozygous for Phe508del. *N Engl J Med* 377: 2013-2023, 2017.

69. **Turner MJ, Saint-Criq V, Patel W, Ibrahim SH, Verdon B, Ward C, Garnett JP, Tarran R, Cann MJ, Gray MA.** Hypercapnia modulates cAMP signalling and cystic fibrosis transmembrane conductance regulator-dependent anion and fluid secretion in airway epithelia. *J Physiol* 594: 1643-1661, 2016.

70. **Uc A, Husted RF, Giriyappa RL, Britigan BE, Stokes JB.** Hemin induces active chloride secretion in Caco-2 cells. *Am J Physiol Gastrointest Liver Physiol* 289: G202-G208, 2005.

71. **Vaandrager AB, Smolenski A, Tilly BC, Houtsmuller AB, Ehlert EME, Bot AGM, Edixhoven M, Boomaars WEM, Lohmann SM, de Jonge HR.** Membrane targeting of cGMP-dependent protein kinase is required for cystic fibrosis transmembrane conductance regulator Cl^- channel activation. *Proc Natl Acad Sci USA* 95: 1466-1471, 1998.

72. **Van Goor F, Hadida S, Grootenhuis PDJ, Burton B, Cao D, Neuberger T, Turnbull A, Singh A, Joubran J, Hazlewood A, Zhou J, McCartney J, Arumugam V, Decker C, Yang J, Young C, Olson ER, Wine JJ, Frizzell RA, Ashlock M, Negulescu P.** Rescue of CF airway epithelial cell function in vitro by a CFTR potentiator, VX-770. *Proc Natl Acad Sci USA* 106: 18825-18830, 2009.

73. **Van Goor F, Yu H, Burton B, Hoffman BJ.** Effect of ivacaftor on CFTR forms with missense mutations associated with defects in protein processing or function. *J Cyst Fibros* 13: 29-36, 2014.

74. **Venglarik CJ, Schultz BD, Frizzell RA, Bridges RJ.** ATP alters current fluctuations of cystic fibrosis transmembrane conductance regulator: evidence for a three-state activation mechanism. *J Gen Physiol* 104: 123-146, 1994.

75. **Wainwright CE, Elborn JS, Ramsey BW, Marigowda G, Huang X, Cipolli M, Colombo C, Davies JC, De Boeck K, Flume PA, Konstan MW, McColley SA, McCoy K, McKone EF, Munck A, Ratjen F, Rowe SM, Waltz D, Boyle MP; TRAFFIC Study Group; TRANSPORT Study Group.** Lumacaftor-ivacaftor in patients with cystic fibrosis homozygous for Phe508del *CFTR*. *N Engl J Med* 373: 220-231, 2015.

76. **Wang F, Zeltwanger S, Yang ICH, Nairn AC, Hwang TC.** Actions of genistein on cystic fibrosis transmembrane conductance regulator channel gating: evidence for two binding sites with opposite effects. *J Gen Physiol* 111: 477-490, 1998.

77. **Wang G.** State-dependent regulation of cystic fibrosis transmembrane conductance regulator (CFTR) gating by a high affinity Fe^{3+} bridge between the regulatory domain and cytoplasmic loop 3. *J Biol Chem* 285: 40438-40447, 2010.

78. **Wang G.** Interplay between inhibitory ferric and stimulatory curcumin regulates phosphorylation-dependent human cystic fibrosis transmembrane conductance regulator and ΔF508 activity. *Biochemistry* 54: 1558-1566, 2015.

79. **Wang G.** Mechanistic insight into the heme-independent interplay between iron and carbon monoxide in CFTR and *Slo1* BK_{Ca} channels. *Metallomics* 9: 634-645, 2017.

80. **Wang R, Wu L.** The chemical modification of K_{Ca} channels by carbon monoxide in vascular smooth muscle cells. *J Biol Chem* 272: 8222-8226, 1997.

81. **Wang S, Publicover S, Gu Y.** An oxygen-sensitive mechanism in regulation of epithelial sodium channel. *Proc Natl Acad Sci USA* 106: 2957-2962, 2009.

82. **Wang W, Li G, Clancy JP, Kirk KL.** Activating cystic fibrosis transmembrane conductance regulator channels with pore blocker analogs. *J Biol Chem* 280: 23622-23630, 2005.

83. **Wang Y, Cai Z, Gosling M, Sheppard DN.** Potentiation of the cystic fibrosis transmembrane conductance regulator Cl^- channel by ivacaftor is temperature independent. *Am J Physiol Lung Cell Mol Physiol* 315: L846-L857, 2018.

84. **Wang Y, Liu J, Loizidou A, Bugeja LA, Warner R, Hawley BR, Cai Z, Toye AM, Sheppard DN, Li H.** CFTR potentiators partially restore channel function to A561E-CFTR, a cystic fibrosis mutant with a similar mechanism of dysfunction as F508del-CFTR. *Br J Pharmacol* 171: 4490-4503, 2014.

85. **Wilkinson WJ, Kemp PJ.** Carbon monoxide: an emerging regulator of ion channels. *J Physiol* 589: 3055-3062, 2011.

86. **Wilson KT, Vaandrager AB, de Vente J, Musch MW, de Jonge HR, Chang EB.** Production and localization of cGMP and PGE_2 in nitroprusside-stimulated rat colonic ion transport. *Am J Physiol Cell Physiol* 270: C832-C840, 1996.

87. **Winter MC, Sheppard DN, Carson MR, Welsh MJ.** Effect of ATP concentration on CFTR Cl^- channels: a kinetic analysis of channel regulation. *Biophys J* 66: 1398-1403, 1994.

88. **Yeh HI, Qiu L, Sohma Y, Conrath K, Zou X, Hwang TC.** Identifying the molecular target sites for CFTR potentiators GLPG1837 and VX-770. *J Gen Physiol* 151: 912-928, 2019.

89. **Zhang RG, Yip CY, Ko WH.** Carbon monoxide inhibits cytokine and chloride secretion in human bronchial epithelia. *Cell Physiol Biochem* 49: 626-637, 2018.

90. **Zhang Z, Liu F, Chen J.** Molecular structure of the ATP-bound, phosphorylated human CFTR. *Proc Natl Acad Sci USA* 115: 12757-12762, 2018.

898 **FIGURE LEGENDS**

899 **Figure 1: CORM-2 inhibits the single-channel activity of CFTR** (*A*) Representative
900 single-channel recordings of wild-type human CFTR in an excised inside-out membrane
901 patch from a C127 cell heterologously expressing CFTR in the absence and presence of the
902 indicated concentrations of CORM-2 added acutely to the intracellular solution. ATP (0.3
903 mM) and PKA (75 nM) were continuously present in the intracellular solution. Dotted lines
904 indicate the closed channel state and downward deflections correspond to channel openings.
905 Unless otherwise indicated in this and other figures, membrane voltage was clamped at –50
906 mV, a large Cl^- concentration gradient was imposed across the membrane patch ($[Cl^-]_{int}$, 147
907 mM; $[Cl^-]_{ext}$, 10 mM) and temperature was 37 °C. (*B*) Single-channel current amplitude
908 histograms for the 10-s recordings shown in *A*. For CORM-2 (1 μM), a small leak current
909 shifted the current amplitude histogram by ~ –0.6 pA relative to that of the control. (*C* and *D*)
910 Concentration-response relationships for CORM-2 inhibition of single-channel current
911 amplitude (*i*) and open probability (P_o) determined from prolonged recordings (≥ 5 minutes)
912 acquired using the conditions described in *A*. Data are means ± SEM (n = 6 – 17). The
913 continuous lines are the fit of sigmoidal 3 parameter functions to mean data.

914

915 **Figure 2: Ruthenium chloride is without effect on the single-channel behavior of CFTR**
916 (*A*) Representative single-channel recordings of wild-type human CFTR in an excised inside-
917 out membrane patch from a C127 cell heterologously expressing CFTR in the absence and
918 presence of $RuCl_3$ (100 μM) added acutely to the intracellular solution. ATP (0.3 mM) and
919 PKA (75 nM) were continuously present in the intracellular solution. Dotted lines indicate
920 the closed channel state and downward deflections correspond to channel openings. (*B* and
921 *C*) Summary single-channel current amplitude (*i*) and open probability (P_o) data determined

922 from prolonged recordings (≥ 5 minutes) show the effects of $RuCl_3$ (100 μM) on wild-type
923 human CFTR. Symbols represent individual values and columns means ± SEM (n = 5).
924
925 **Figure 3: CORM-3 inhibits the single-channel activity of CFTR** (*A*) Representative
926 single-channel recordings of wild-type human CFTR in an excised inside-out membrane
927 patch from a C127 cell heterologously expressing CFTR in the absence and presence of the
928 indicated concentrations of CORM-3 and $CFTR_{inh}$-172 added acutely to the intracellular
929 solution. ATP (0.3 mM) and PKA (75 nM) were continuously present in the intracellular
930 solution. Dotted lines indicate the closed channel state and downward deflections correspond
931 to channel openings. (*B*) Single-channel current amplitude histograms for the 10-s recordings
932 shown in *A*. With the exception of CORM-3 (300 μM) where the leak current was ~ –4.8 pA,
933 in the presence of CORM-3 a small leak current shifted the current amplitude histogram by ~
934 –0.6 pA relative to that of the control. (*C* and *D*) Summary single-channel current amplitude
935 (*i*) and open probability (P_o) data determined from prolonged recordings (≥ 5 minutes) show
936 the effects of CORM-3 (30 – 300 μM) and $CFTR_{inh}$-172 (I172; 10 μM) on wild-type human
937 CFTR. Symbols represent individual values and columns means ± SEM (n = 5 – 6); **, P <
938 0.01; ***, P < 0.001 vs control.
939
940 **Figure 4: Dwell time histograms of a single CFTR Cl^- channel inhibited by CORM-2** (*A*
941 and *B*) Representative dwell-time histograms for a single wild-type human CFTR Cl^- channel
942 recorded in the absence (*A*) and presence (*B*) of CORM-2 (30 μM) in the intracellular
943 solution; ATP (0.3 mM) and PKA (75 nM) were present throughout the recordings. The
944 continuous lines are the fit of one-, two- or four-component exponential functions to the data
945 and the dashed lines show the individual components of these functions. The vertical dashed

946 lines indicate mean values of the different time constants (for details, see Table 1).
947 Logarithmic *x*-axes with 10 bins decade^{-1} were used for dwell-time histograms.
948
949 **Figure 5: CFTR inhibition by CORM-2 is voltage-independent** (*A*) Representative
950 recordings of two wild-type human CFTR Cl^- channels in an excised inside-out membrane
951 patch from a C127 cell heterologously expressing CFTR. The recordings were acquired at
952 ±50 mV in the absence and presence of CORM-2 (30 μM). ATP (0.3 mM) and PKA (75 nM)
953 were continuously present in the intracellular solution and the membrane patch was bathed in
954 symmetrical 147 mM Cl^- solutions. Dotted lines indicate the closed channel state and
955 downward deflections at –50 mV and upward deflections at +50 mV correspond to channel
956 openings, identified by the labels O1 and O2. (*B* and *C*) Summary single-channel current
957 amplitude (*i*) and open probability (P_o) data show the effects of CORM-2 (30 μM) on wild-
958 type human CFTR at ±50 mV. Symbols represent individual values and columns means ±
959 SEM ($n = 6$); **, $P < 0.01$ vs. control.
960
961 **Figure 6: The ATP-dependence of CFTR inhibition by CORM-2** (*A* and *B*)
962 Representative recordings of wild-type human CFTR Cl^- channels in excised inside-out
963 membrane patches from C127 cells heterologously expressing CFTR in the absence and
964 presence of CORM-2 (30 μM) when the ATP concentration was either 0.3 mM (*A*) or 3 mM
965 (*B*). ATP (0.3 or 3 mM) and PKA (75 nM) were continuously present in the intracellular
966 solution. Dotted lines indicate the closed channel state and downward deflections correspond
967 to channel openings. (*C* and *D*) Summary single-channel current amplitude (*i*) and open
968 probability (P_o) data determined from prolonged recordings (≥ 5 minutes) show the effects of
969 CORM-2 (30 μM) on wild-type human CFTR when the intracellular solution contained either

970 0.3 or 3 mM ATP. Symbols represent individual values and columns means ± SEM (n = 6 –
971 8); *, $P < 0.05$ vs. control at same [ATP].
972
973 **Figure 7: Ivacaftor impedes CFTR inhibition by CORM-2** (*A*) Representative single-
974 channel recordings of wild-type human CFTR in an excised inside-out membrane patch from
975 a C127 cell heterologously expressing CFTR under the indicated experimental conditions.
976 Small molecules were acutely added to the intracellular solution in the continuous presence of
977 ATP (0.3 mM) and PKA (75 nM). Dotted lines indicate the closed channel state and
978 downward deflections correspond to channel openings. (*B* – *E*) Summary single-channel
979 current amplitude (*i*), open probability (P_o), mean burst duration (MBD) and interburst
980 interval (IBI) data determined from prolonged recordings (≥ 5 minutes) show the effects
981 CORM-2 (30 μM) and $CFTR_{inh}$-172 (10 μM) on wild-type human CFTR potentiated by
982 ivacaftor (100 nM); compounds were added sequentially and cumulatively. Symbols
983 represent individual values and columns means ± SEM (n = 4 – 6); **, $P < 0.01$; ***, $P <$
984 0.001 vs. control.
985
986 **Figure 8: Ivacaftor relieves CFTR inhibition by CORM-2** (*A* and *B*) Summary single-
987 channel current amplitude (*i*) and open probability (P_o) data determined from prolonged
988 recordings (≥ 5 minutes) show the effects of ivacaftor (100 nM) and $CFTR_{inh}$-172 (10 μM) on
989 wild-type human CFTR inhibited by CORM-2 (30 μM); compounds were added sequentially
990 and cumulatively. Symbols represent individual values and columns means ± SEM (n = 5);
991 **, $P < 0.01$; ***, $P < 0.001$ vs. control.
992

TABLES

Table 1: Effects of CORM-2 on the open- and closed-time constants of wild-type human CFTR

	[CORM-2] (μM)	
[Drug]	0	30
n	3	3
τ_{O1} (ms)	-----	11.4 ± 5.2
τ_{O2} (ms)	35.7 ± 8.8	42.6 ± 24.6
τ_{C1} (ms)	-----	0.75 ± 0.49
τ_{C2} (ms)	2.22 ± 0.04	3.51 ± 0.71
τ_{C3} (ms)	196 ± 44	115 ± 32
τ_{C4} (ms)	-----	2,225 ± 1,255
Area under curve τ_{O1}	-----	0.67 ± 0.14
Area under curve τ_{O2}	1	0.33 ± 0.14
Area under curve τ_{C1}	-----	0.51 ± 0.23
Area under curve τ_{C2}	0.75 ± 0.05	0.37 ± 0.19
Area under curve τ_{C3}	0.25 ± 0.05	0.11 ± 0.04
Area under curve τ_{C4}	-----	0.01 ± 0.01
Events per minute	1,136 ± 204	1,071 ± 267
Total time (s)	1,442	845

Table 1: Effects of CORM-2 on the open- and closed-time constants of wild-type human CFTR Open- and closed-time constants were measured at the indicated concentrations of CORM-2 by fitting one-, two- or four-component exponential functions to open- and closed-time histograms. Areas under curve indicate the proportion of the total dwell time distribution that correspond to the different time constants. Events per minute represents the number of transitions between the open and closed states within one minute. The total time analyzed in the absence and presence of CORM-2 (30 μM) is shown and in each membrane patch ~5,000 events were analyzed per intervention. Values are means ± SEM of *n* observations. Measurements were made in the presence of the catalytic subunit of PKA (75 nM) and ATP (0.3 mM) in the intracellular solution. Voltage was –50 mV, there was a large Cl^- concentration gradient across the membrane patch ($[Cl^-]_{internal}$ = 147 mM; $[Cl^-]_{external}$ = 10 mM) and temperature was 37 °C.

Figure 1

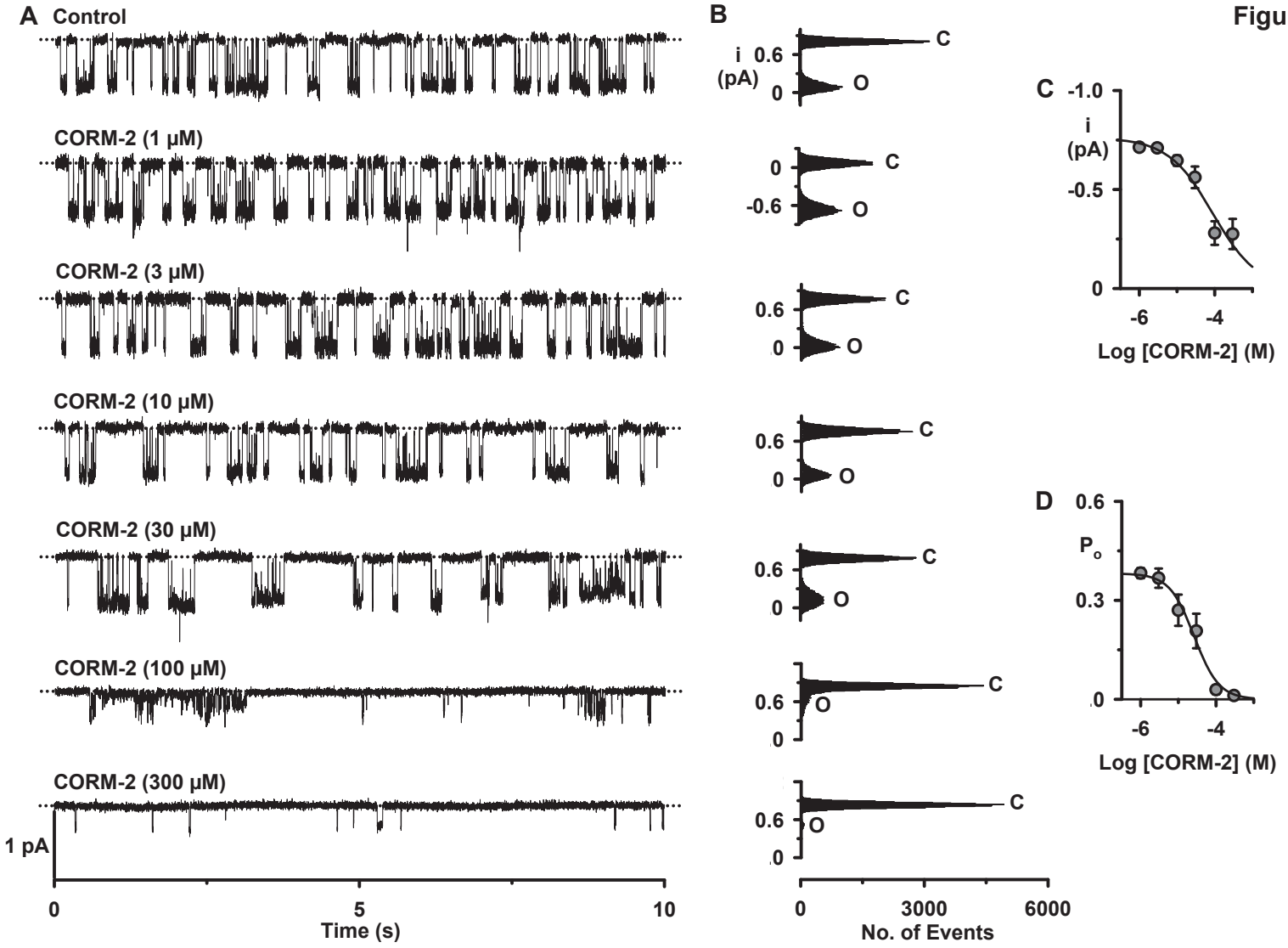
A
Control
CORM-2 (1 μM)
CORM-2 (3 μM)
CORM-2 (10 μM)
CORM-2 (30 μM)
CORM-2 (100 μM)
CORM-2 (300 μM)
1 pA
0
5
10
Time (s)
B
i (pA)
0.6
0
C
O
-0.6
No. of Events
0
3000
6000
C
-1.0
-0.5
-6
-4
Log [CORM-2] (M)
D
P_o
0.3

Figure 2

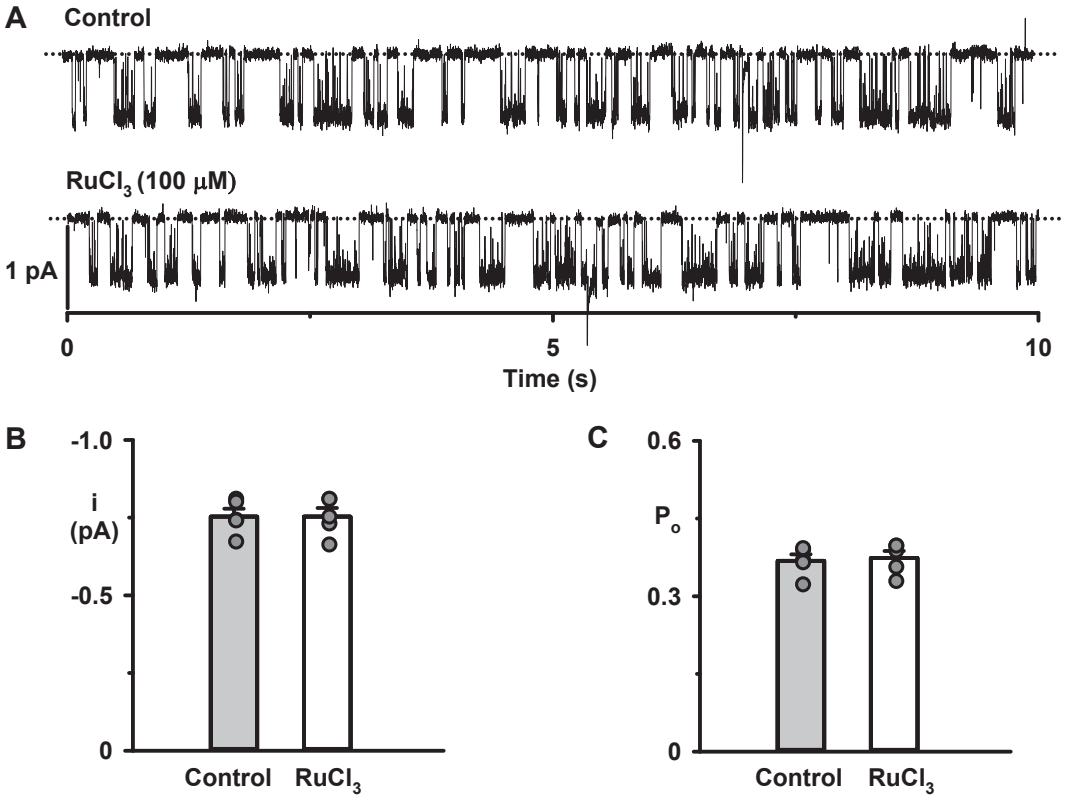
A
Control
RuCl3 (100 μM)
1 pA
0
5
10
Time (s)
B
-1.0
i
(pA)
-0.5
0
Control
RuCl3
C
0.6
Po
0.3
0
Control
RuCl3

Figure 3

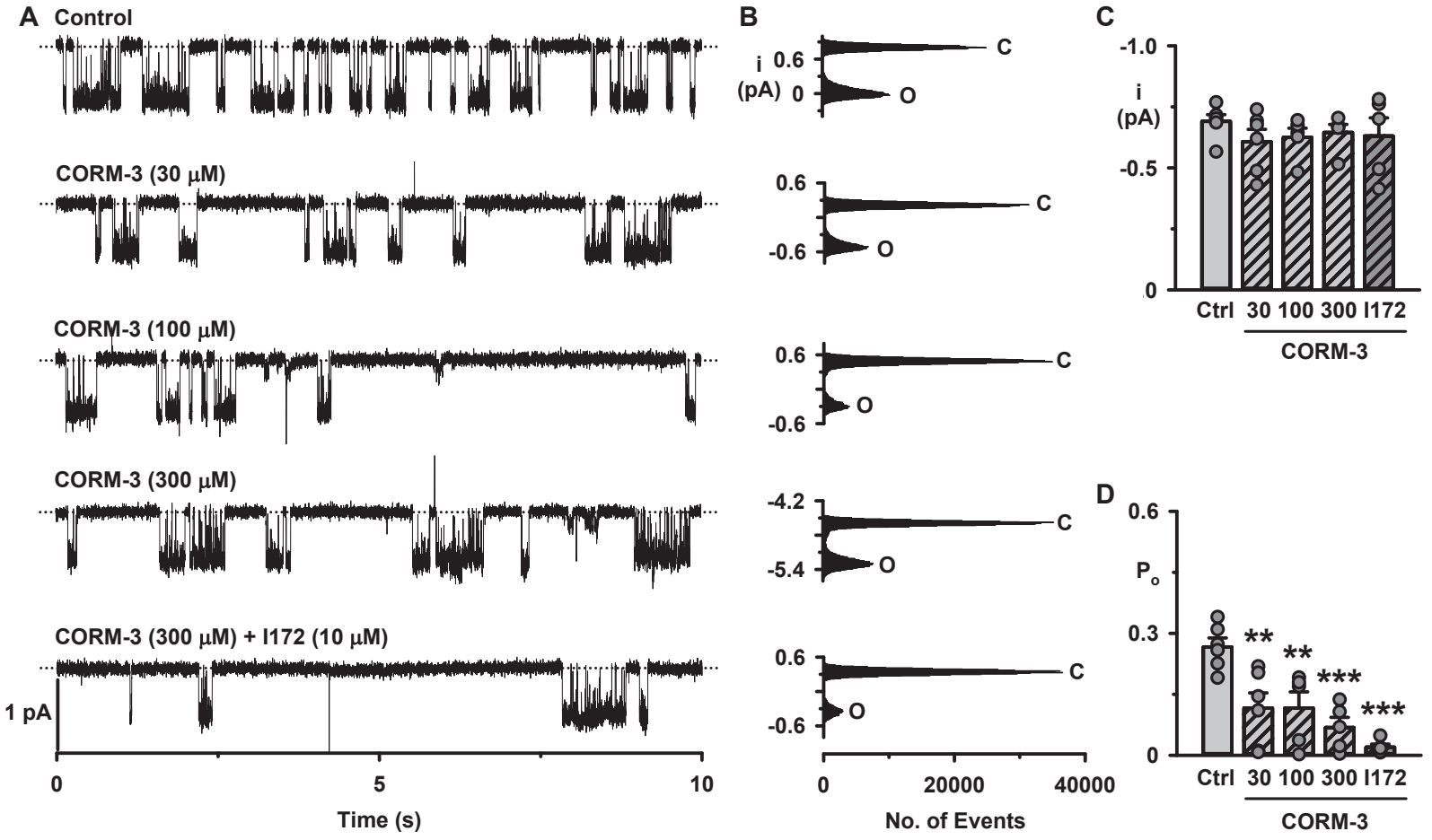
A
Control
CORM-3 (30 μM)
CORM-3 (100 μM)
CORM-3 (300 μM)
CORM-3 (300 μM) + I172 (10 μM)
1 pA
0
5
10
Time (s)
B
i (pA)
0.6
0
C
O
0.6
-0.6
-4.2
-5.4
0
20000
40000
No. of Events
C
-1.0
-0.5
0
Ctrl
30
100
300
I172
CORM-3
D
0.6
0.3
0
Po
**
***

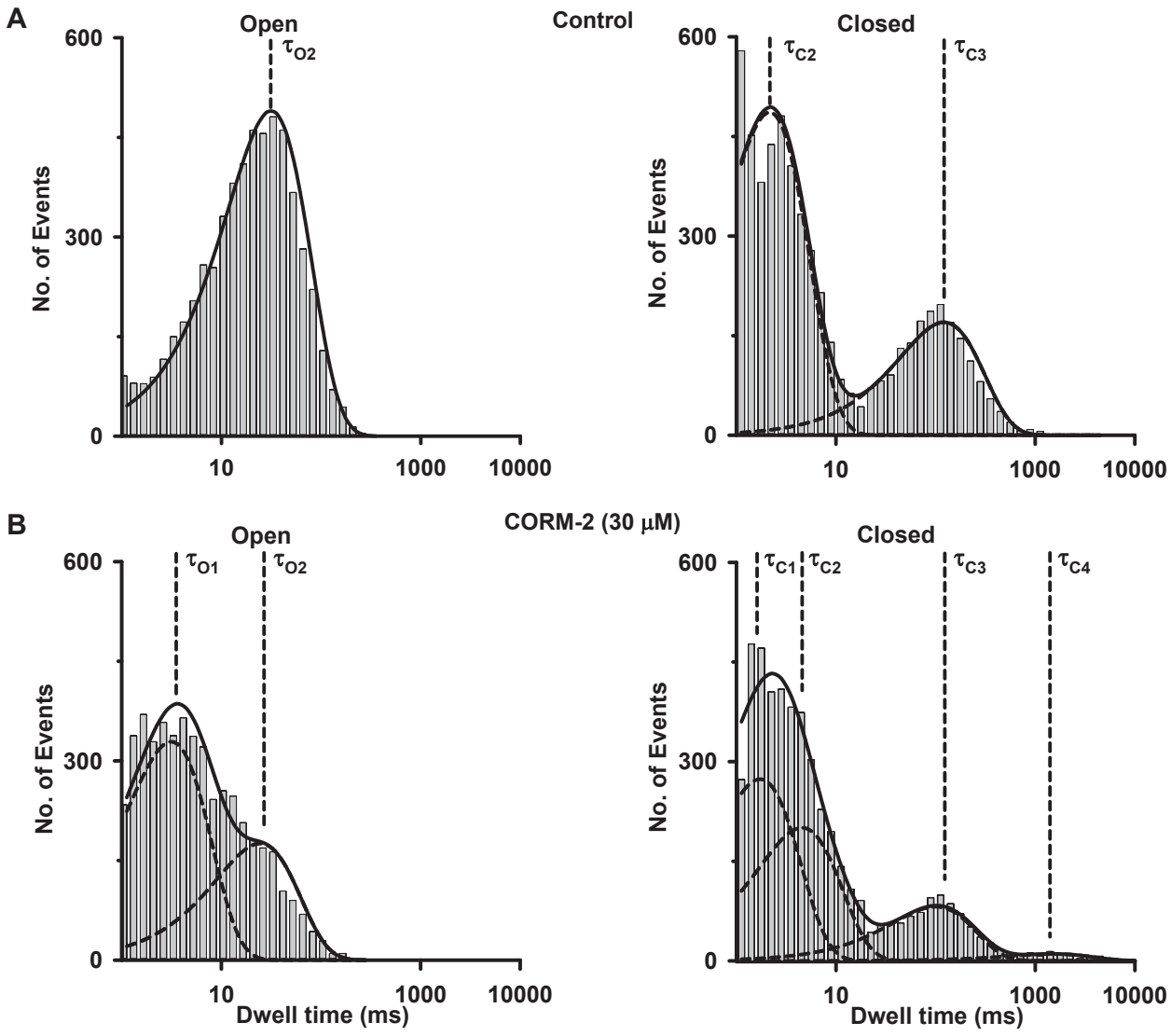
A
Control
Open
τ_{O2}
600
300
0
No. of Events
10
1000
10000
Closed
τ_{C2}
τ_{C3}
B
CORM-2 (30 μM)
Open
τ_{O1}
τ_{O2}
Dwell time (ms)
Closed
τ_{C1}
τ_{C2}
τ_{C3}
τ_{C4}

Figure 4

Figure 5

A

-50 mV Control

-50 mV CORM-2

C

O1

O2

1 pA

+50 mV Control

+50 mV CORM-2

O2

O1

C

0

5

10

Time (s)

0

5

10

Time (s)

B

Control

CORM-2

-1.0

i (pA)

-0.5

0

-50 mV

1.0

i (pA)

0.5

0

+50 mV

C

0.6

P_o

0.3

0

**

-50 mV

0.6

P_o

0.3

0

**

+50 mV

Figure 6

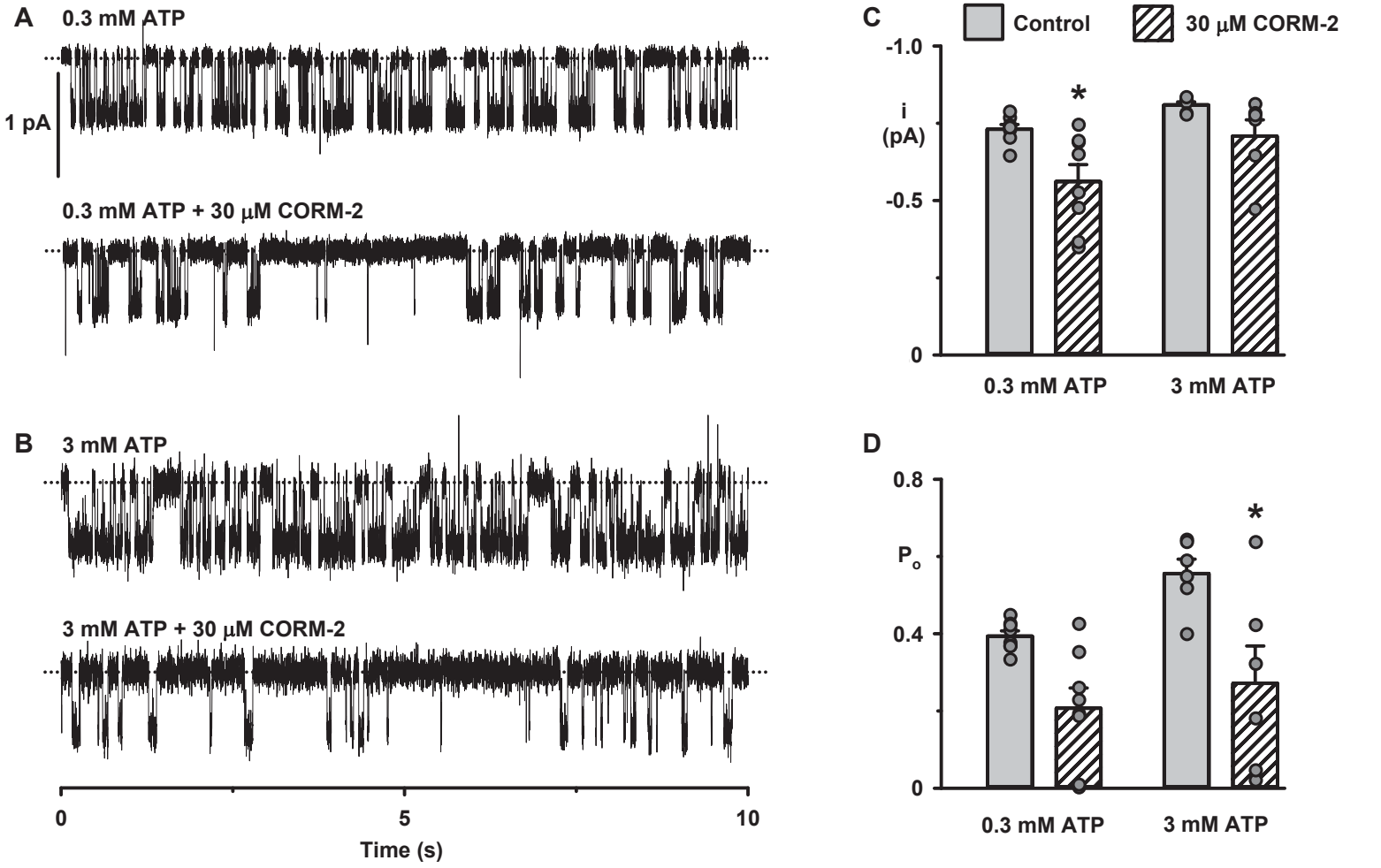
A
0.3 mM ATP
1 pA
0.3 mM ATP + 30 μM CORM-2
B
3 mM ATP
3 mM ATP + 30 μM CORM-2
0
5
10
Time (s)
C
Control
30 μM CORM-2
-1.0
i
(pA)
-0.5
0
*
0.3 mM ATP
3 mM ATP
D
0.8
P o
0.4
0
*
0.3 mM ATP
3 mM ATP

Figure 7

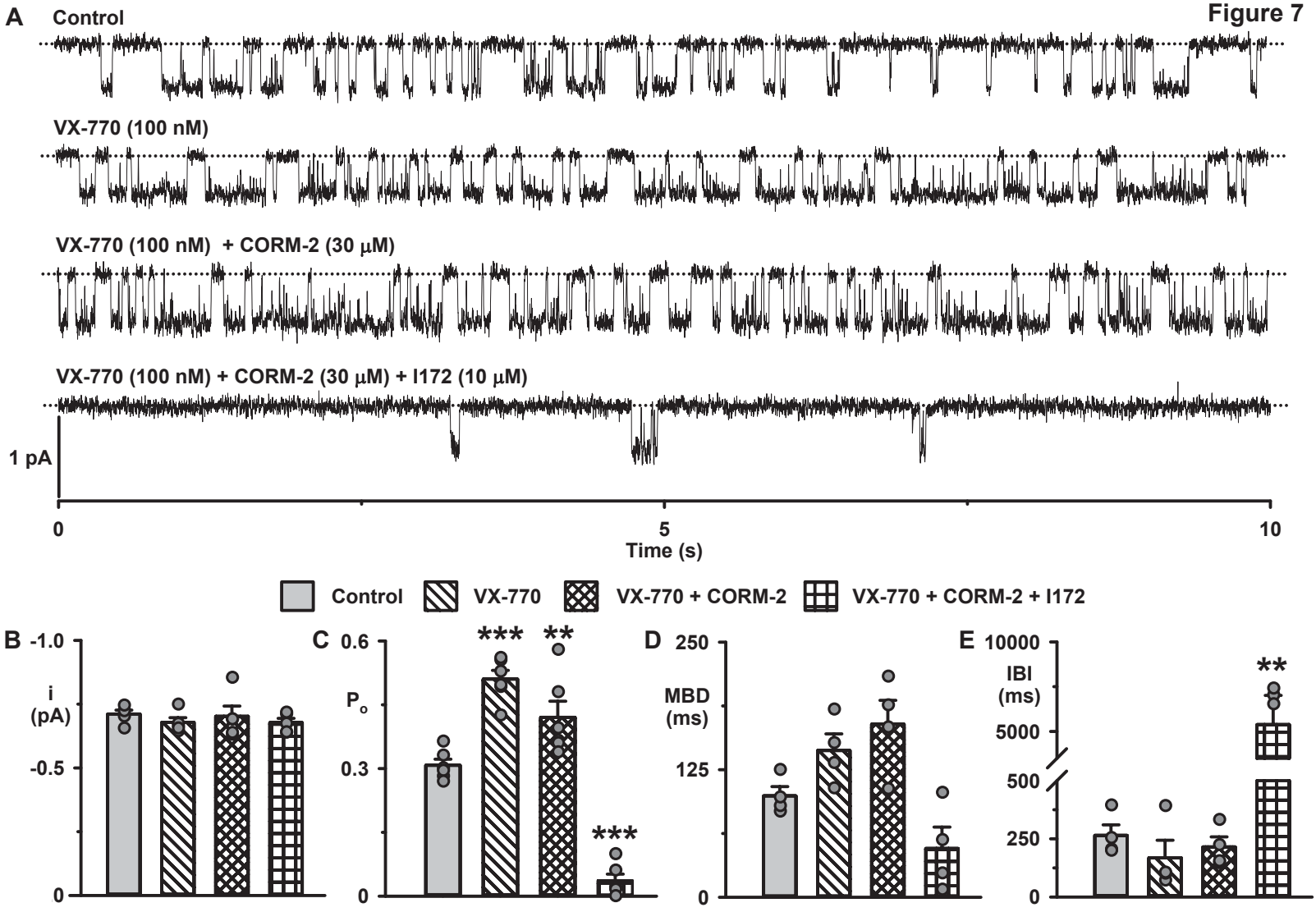
A
Control
VX-770 (100 nM)
VX-770 (100 nM) + CORM-2 (30 μM)
VX-770 (100 nM) + CORM-2 (30 μM) + I172 (10 μM)
1 pA
0
5
10
Time (s)
Control
VX-770
VX-770 + CORM-2
VX-770 + CORM-2 + I172
B
-1.0
i (pA)
-0.5
0
C
0.6
Po
0.3
0
***
**
***
D
250
MBD (ms)
125
0
E
10000
IBI (ms)
5000
500
250
0
**

Figure 8

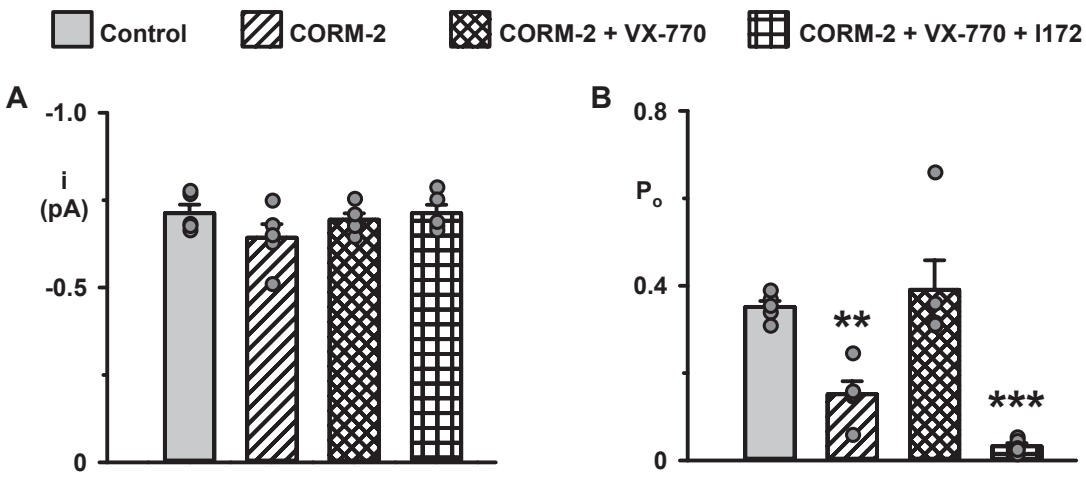
Control
CORM-2
CORM-2 + VX-770
CORM-2 + VX-770 + I172
A
-1.0
i
(pA)
-0.5
0
B
0.8
Po
0.4
0
**
***